Response to Tilted Magnetic Fields in Bi 2 Sr 2 CaCu 2 O 8 with Columnar Defects: Evidence for Transverse Meissner Effect

V. Ta Phuoc, Enrick Olive, R. de Sousa, A. Ruyter, L. Ammor, J. Soret

Response to Tilted Magnetic Fields in $Bi_2Sr_2CaCu_2O_8$ with Columnar Defects: Evidence for Transverse Meissner Effect

V. Ta Phuoc, E. Olive, R. De Sousa, A. Ruyter, L. Ammor, and J. C. Soret
LEMA, CNRS-FRE 2077, Université François Rabelais, 37200 Tours, France
(Received 19 January 2001; published 18 April 2002)

The transverse Meissner effect (TME) in the highly layered superconductor $Bi_2Sr_2CaCu_2O_{8+y}$ with columnar defects is investigated by transport measurements. We present evidence for the persistence of the Bose glass phase for $H_\perp < H_{\perp c}$: (i) the variable-range vortex hopping process crosses over to the half-loop regime; (ii) near $H_{\perp c}$ the energy barriers vanish linearly with $H_\perp$; (iii) the transition temperature is governed by $T_{\rm BG}(H_\parallel, 0) - T_{\rm BG}(H_\parallel, H_\perp) \sim |H_\perp|^{1/\nu_\perp}$ with $\nu_\perp = 1.0 \pm 0.1$. Furthermore, above the transition as $H_\perp \rightarrow H^+_{\perp c}$, moving kink chains consistent with a commensurate-incommensurate transition scenario are observed. These results show the existence of the TME for $H_\perp < H_{\perp c}$.

DOI: 10.1103/PhysRevLett.88.187002 PACS numbers: 74.60.Ge, 74.72.Hs

The interplay between elasticity, interactions, thermal fluctuations, and dimensionality of magnetic flux lines subject to pinning yields a large variety of vortex phases in high-T_c superconductors [1]. The nature of these phases and how they depend on the pinning is far from being completely elucidated. The theory of pinning by correlated disorder, such as twin planes or amorphous columnar tracks created by heavy ions, has been considered by Nelson and Vinokur (NV) [2] and Hwa *et al.* [3]. In the case of parallel tracks, NV have shown that, if the applied magnetic field **H** is aligned with the columnar defects, the low temperature physics of vortices is similar to that of the Bose glass (BG) [4], with the flux lines strongly localized in the tracks leading to zero creep resistivity. When **H** is tilted at an angle θ away from the column direction, the BG phase with perfect alignment of the internal flux density **B** parallel to the columns is predicted to be stable up to a critical transverse field $H_{\perp c}$ producing the so-called transverse Meissner effect (TME) [2,5]. For $\theta > \theta_c \equiv \arctan(\mu_0 H_{\perp c}/B)$, the linear resistivity is finite resulting from the appearance of kink chains along the transverse direction as discussed in Ref. [6]. Finally, above a still larger angle, the kinked vortex structures disappear and **B** becomes collinear with **H**. Similar scenarios apply to vortex pinning by the twin boundaries [2] and by the layered structure of the compound itself [7].

Recently, the TME in untwinned single crystals of $YBa_2Cu_3O_7$ (YBCO) with columnar defects has been observed using Hall sensors [8]. Previous magnetic measurements in anisotropic 3D superconductors, such as YBCO, gave support to the presence of vortex lock-in phenomena, due to pinning by the twin boundaries [9] or by the interlayers between the Cu-O planes [10]. In the case of highly layered superconductors, such as $Bi_2Sr_2CaCu_2O_{8+y}$ (BSCCO), the lock-in transition was observed for **H** tilted away from the layers [11], but the existence of the TME due to the pinning by columnar defects remained an open question.

In this Letter, we present measurements of the electrical properties near the glass-liquid transition in BSCCO single crystals with parallel columnar defects, as a function of T and θ for filling factors $f \equiv \mu_0 H_\parallel / B_\Phi < 1$. Below a critical angle $\theta_c(T)$, we observe a vanishing resistivity $\rho(J)$ for low currents. A detailed *quantitative* analysis of $\rho(J)$ indicates that the creep proceeds via variable-range vortex hopping (VRH) at low currents due to some disorder [12], crossing over to the half-loop (HL) regime at high currents. For $\theta > \theta_c(T)$, the very signature of a kinked vortex structure, consistent with a commensurate-incommensurate (CIC) transition scenario in $1 + 1$ dimensions [6], is deduced from the critical behavior of the linear resistivity. All these results clearly demonstrate that, when **H** is tilted at $\theta < \theta_c$ away from the defects, the flux lines remain localized on columnar defects, and hence the BG exhibits a TME.

The BSSCO single crystal was grown by a self-flux technique, as described elsewhere [13]. The crystal of $1 \times 1 \times 0.030$ mm^3 size with the c axis along the shortest dimension has a T_c of 89 K, a transition width of $\sim$1 K, and was irradiated along its c axis with 5.8 GeV Pb ions to a dose corresponding to $B_\Phi = 1.5$ T at the GANIL (France). Isothermal I-V curves were recorded using a dc four-probe method with a sensitivity of $\sim 10^{-10}$ V and a temperature stability better than 5 mK. **H** was aligned with the tracks using the well-known dip feature occurring in the dissipation process for $\theta = 0°$, and was tilted with an angular resolution better than 0.1° away from the column direction for f fixed.

Figure 1 shows a typical log-log plot of V/I-I curves obtained by varying θ for $f = 1/3$ and T fixed below the BG transition temperature determined at $\theta = 0°$ [12]. We observe a well-defined angular crossover at an angle θ_c. For $\theta < \theta_c$, the data suggest that the BG phase persists. On the contrary, the existence of an Ohmic regime for $\theta > \theta_c$ indicates a liquid vortexlike state.

We first focus on the angular range $\theta < \theta_c$, and we consider the scenario where the BG phase is stable. Thus,

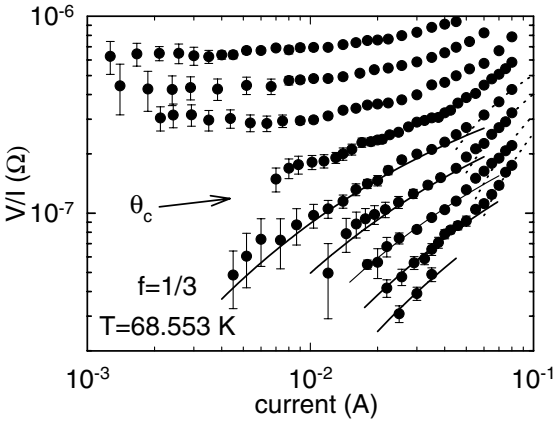

FIG. 1. V/I-I curves for tilted magnetic fields. From the right to the left $\theta = 0°$, 5°, 10°, 15°, 20°, 25°, 30°, 35°, and 40°. The curved lines are a fit of the Bose glass theory to the data.

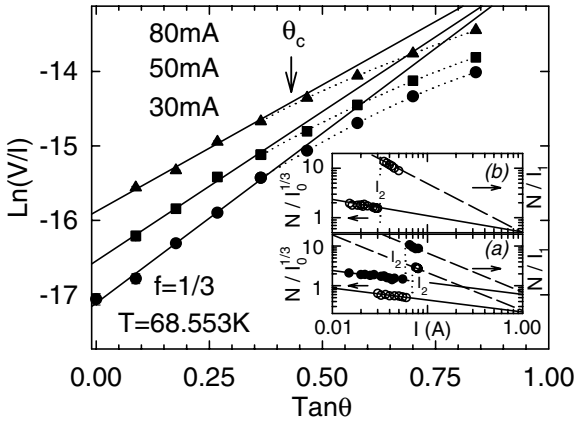

FIG. 2. Angular dependence of $\ln(V/I)$ for different I. The solid lines are a fit of $\ln(V/I) = M + N\tan\theta$ to the data; the dotted lines are a guide for the eye. Inset: $N/I_0^{1/3}$ vs I (left axis) and N/I_1 vs I (right axis) with I_0 and I_1 determined from theory. Inset (a): $f = 1/3$ and $T = 68.553$ K (filled symbols), $f = 2/15$ and $T = 69.136$ K (open symbols). Inset (b): $f = 1/3$ and $T = 59.960$ K in another crystal with $B_\Phi = 0.75$ T. The straight lines are fits whence we obtain $\mu = 0.33 \pm 0.05$ (solid line) for $I < I_2$ and $\mu = 1.0 \pm 0.1$ (dashed line) for $I > I_2$.

one expects that excitations of some localized vortex lines lead to a nonlinear resistivity given by [2]

$$\rho(J) = \rho_0 \exp[-\tilde{E}_K(J_c/J)^\mu/k_BT], \qquad (1)$$

where ρ_0 is a characteristic flux-flow resistivity and $\tilde{E}_K(J_c/J)^\mu$ represents the barriers against vortex motion. This expression is predicted to hold for various regimes of different behavior as the current probes different length scales in the BG. $\tilde{E}_K$ acts as a scaling parameter for the pinning energy and J_c is the characteristic current scale of the creep process. When the current is large enough that the growth of vortex-loop excitations of a line from its pinning track does not reach out to the neighboring tracks, the HL excitations are relevant and yield an exponent $\mu = 1$ and $J_c \equiv J_1 = U/(\Phi_0 d)$, where U is the mean pinning potential and $d = \sqrt{\Phi_0/B_\Phi}$ is the mean spacing between pins. With decreasing current, the size of half-loops increases with the result that some disorder in the pinning potential becomes relevant. This situation yields the VRH process characterized by $\mu = 1/3$ and by another important current scale $J_c \equiv J_0 = 1/[\Phi_0 g(\tilde{\mu})d^3]$, where $g(\tilde{\mu})$ denotes the density of pinning energies at the chemical potential of the vortex system. One expects that both J_1 and J_0 are insensitive to $H_\perp$. We therefore consider that the only important effect of $H_\perp$ is to lower $\tilde{E}_K$, according to the formula

$$\tilde{E}_K = E_K - \epsilon^2\Phi_0 d H_\perp, \qquad (2)$$

where E_K is the mean kink energy, and the energy gain due to the tilt is obtained from the isotropic result $\Phi_0 d H_\perp$ by applying the scaling rule [Eq. (3.12)] of Ref. [1].

We now present the following two-step method of fitting Eqs. (1) and (2) to the data, which allows us to obtain a good understanding of the physics in our experiment. First, we plot in Fig. 2 the natural logarithm of V/I versus $\tan\theta$ for I fixed. Note that $\tan\theta$ is here directly proportional to $H_\perp$ since f is kept constant. A linear variation $\ln(V/I) = M + N\tan\theta$ (expression designated below as $E1$) with M and N being current-dependent parameters is found for θ varying up to θ_c (solid lines), whereas above θ_c the data deviate from this behavior (dotted lines). This finding is another argument supporting a true angular transition at θ_c, as suggested in Fig. 1. It should be noted that we draw such a conclusion from the observation of two *independent* regimes of *different* behavior. One leads to a vanishing linear resistivity as $\theta \to \theta_c^+$, and the other is evidenced by probing the regions of nonlinear resistivity above and below θ_c. Another result is that $N \sim I^{-\mu}$ with μ undergoing a jump from 1/3 to 1 at $I_2 \approx 60$ mA. Such a current crossover is clearly visible in inset a of Fig. 2 (filled symbols), where we plot together N normalized by $I_0^{1/3}$ and N normalized by I_1 versus I depending upon whether I is $<I_2$ or $>I_2$, respectively. Here, I_0 and I_1 are two currents evaluated on the basis of the BG model, as will be seen below. It therefore follows that $N_{1/3}(I) = K(I_0/I)^{1/3}$ and $N_1(I) = KI_1/I$, where the labels 1/3 and 1 differentiate between two fits below and above I_2, respectively. In both these equations, $K \approx 0.6$ is a dimensionless constant. It should be noted that such a crossover at I_2 is clearly observed from V/I-I curves as well (see Fig. 1), where a sudden increase of V/I, suggesting an increasing vortex motion, occurs at I_2. Second, we plot in Fig. 3 and its inset the natural logarithm of V/I versus $I^{-1/3}$ for $I < I_2$ and I^{-1} for $I > I_2$, respectively. We verify that the expression $\ln(V/I) = P - Q_\mu I^{-\mu}$ (expression designated below as $E2$) fits very well our experimental data (solid lines) with an exponent $\mu = 1/3$ for $I < I_2$ and with $\mu = 1$ for $I > I_2$. In $E2$, Q_μ is labeled using the above convention. The result is that P is a constant (within the experimental errors), while Q_μ depends

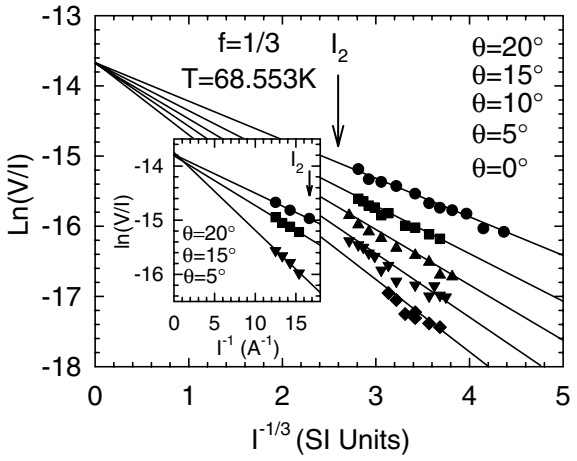

FIG. 3. $\ln(V/I)$ vs $I^{-1/3}$ for $I < I_2$ and $\theta < \theta_c$. Inset: $\ln(V/I)$ vs I^{-1} for $I > I_2$ and $\theta < \theta_c$. In both plots the lines are a fit to the data using the form $\ln(V/I) = P - Q_\mu I^{-\mu}$ with $\mu = 1/3$ or 1 according to whether I is $<I_2$ or $>I_2$.

on θ. In Fig. 4 and its lower inset, we show $Q_{1/3}$ and Q_1 versus $\tan\theta$, respectively. A linear variation in $\tan\theta$ is observed consistently with expression $E1$. In the upper inset of Fig. 4, we plot together $Q_{1/3}/I_0^{1/3}$ and Q_1/I_1 versus $\tan\theta$. The result is that the data are superimposable onto a single straight line with slope ≈ -0.6 consistent with the value of $-K$, as may be verified by identifying the expression $E1$ with the expression $E2$.

In conclusion, $V/I = R_0 \exp[-(K' - K\tan\theta) \times (I_0/I)^{1/3}]$ is clearly observed in our experiment for $I < I_2$ (solid lines in Fig. 1) while $V/I = R_0 \times \exp[-(K' - K\tan\theta)(I_1/I)]$ is valid for data above I_2 (dashed lines in Fig. 1). In both fitting expressions, K and K' depend on f and T. In the case of data presented in Fig. 1, $K \approx 0.6$ and $K' \approx 0.4$; furthermore $I_0 = 15$ A and $I_1 = 0.4$ A are evaluated from the BG model (see below), and $R_0 \approx 1.1\ \mu\Omega$ is 5 orders of magnitude lower than the normal resistance. Therefore, for $\theta < \theta_c$ we have rather strong evidence of two separate (albeit related) vortex creep processes peculiar to a BG: the HL expansion with $\mu = 1$ which is cut off by the crossover at I_2 into the VRH process with $\mu = 1/3$. Moreover, we note that, for each filling factor investigated in our experiment ($f = 2/15$, $1/3$, $2/3$), we observe a *continuation* of the VRH process evidenced at $\theta = 0°$ [12]. We therefore argue that the BG phase remains stable up to a critical tilting angle θ_c, as predicted by NV [2].

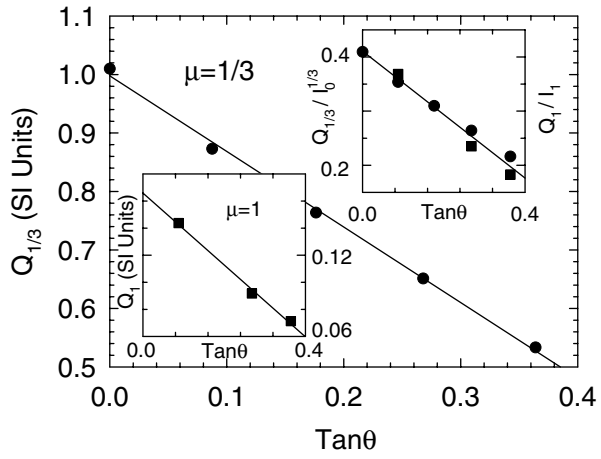

FIG. 4. Angular dependence of $Q_{1/3}$ defined in the regime $I < I_2$ (see Fig. 3). Lower inset: angular dependence of Q_1 defined in the regime $I > I_2$. Upper inset: angular dependence of $Q_{1/3}/I_0^{1/3}$ and Q_1/I_1. In each plot the straight line is a least-squares fit.

To test the accuracy of the above view, we first estimate from the theory [1,2] the characteristic current scales, second the current crossover, and third the energy barriers in Eq. (1). J_0 depends only on $g(\tilde{\mu})$, the density of pinning energies evaluated at the chemical potential of the vortex system. Although a form of $g(x)$ is not yet available, an estimate of $g(\tilde{\mu})$ can be done in terms of the bandwidth of pinning energies γ, due to the disorder, and hence $g(\tilde{\mu}) \approx 1/(d^2\gamma)$ so that $J_0 \approx \gamma/\phi_0 d$. Following Blatter *et al.* [1], $\gamma = t_d + \gamma_i$, where $t_d \approx U/\sqrt{E_K/k_BT}\exp(-\sqrt{2}\,E_K/k_BT)$ estimates the dispersion in the pinning energies resulting from disorder in the position of tracks [2] and γ_i arises from some on-site randomness. We shall assume random defect radii as the main source of on-site disorder. A reasonable estimate of γ_i is then given by the width of the distribution of pinning energies $\tilde{P}(U_K) = P(c_K)dc_K/dU_K$, where U_K is the binding energy of a defect with radius c_K and $P(c_K)$ is the probability distribution of the defect radii. A realistic pdf is a normal law centered at $c_0 = 45$ Å with a standard deviation of 6 Å, as shown in Fig. 1 of Ref. [12]. Thus, by using the formula $U_K = (\phi_0^2/8\pi\mu_0\lambda_{ab}^2)\ln[1 + (c_K/\sqrt{2}\,\xi_{ab})^2]$ [1,2] where λ_{ab} and ξ_{ab} are, respectively, the planar penetration depth and the planar coherence length, we determine $U_0 = \langle U_K\rangle$ representing the energy scale for the vortex pinning. Another important energy scale corresponding to vortex positional fluctuations is $T^\star = (k_B c_0/4\xi_0 G_i)\sqrt{\ln(a_0/\xi_{ab})}\,(T_c - T)$, where G_i is the 2D Ginzburg number and $a_0 = \sqrt{\phi_0/B}$ is the vortex-lattice constant. U_0 and $T^\star$ completely characterize the system of vortices and columnar defects. Thus, it can be inferred that $E_K = (d/\sqrt{2}\,\xi_{ab})T^\star\sqrt{f(T/T^\star)}$, where $f(x) = x^2/2\exp(-2x^2)$ accounts for entropic effects, and $U = U_0 f(T/T^\star)$. Using appropriate parameters for BSCCO ($\lambda_0 \approx 1850$ Å, $\xi_0 \approx 20$ Å, and $G_i \approx 0.2$) we estimate $J_0 \approx 10^9$ A/m^2 and $J_1 \approx 2.6 \times 10^7$ A/m^2 for $f = 1/3$ and $T = 68$ K, respectively. The balance between the barrier energy for the VRH process $U_{\mathrm{VRH}} = \tilde{E}_K(J_0/J)^{1/3}$ and the barrier for the HL regime $U_{\mathrm{HL}} = \tilde{E}_K J_1/J$ determines the crossover current $J_2 = (J_1/J_0)^{1/2}J_1 = U^{3/2}/(\phi_0 d\sqrt{\gamma})$. Thus, we have $J_2 \ll J_1 \ll J_0$, so that the crossover between the VRH process and the HL regime takes place at J_2. Assuming uniform currents in the sample, we find $I_2 \approx 60$ mA, in excellent agreement with

the experiment (Fig. 1). A more complete quantitative evaluation of the consistency of the data with the model is obtained for different values of f and T, as well as for different values of d (inset of Fig. 2). In particular, we find that the effect of d on I_2 is in good agreement with the prediction $I_2 \propto 1/d$. Finally, evaluating U_{VRH} and U_{HL} with $\tilde{E}_K$ from Eq. (2), we find, using again the above usual parameters of BSCCO with $\epsilon \approx 1/200$, that $E_K/k_BT \approx 0.3$ and $\varepsilon^2\phi_0 dH_\perp/k_BT \approx 0.7\tan\theta$ for $f = 1/3$ and $T = 68$ K, which correspond to the values of our fitting parameters K' and K (see upper inset of Fig. 4). Thus, the experiment is also in good agreement with the barriers U_{VRH} and U_{HL} theoretically predicted below and above I_2, respectively.

Finally, we proceed to the linear regime observed above θ_c (see Fig. 1). For $\theta > \theta_c$, Hwa *et al.* [6] predict, on the basis of the CIC transition, the appearance of free moving chains of kinks oriented in the $H_\perp$ direction leading to a critical behavior of the linear resistivity $\rho \sim (\tan\theta - \tan\theta_c)^\nu$ characterized by an exponent $\nu = 1/2$ ($\nu = 3/2$) in 1 + 1 (2 + 1) dimensions. This type of behavior with $\nu = 1/2$ is evident in Fig. 5 which shows a plot of R/R_c versus $\tan\theta - \tan\theta_c$ for different values of f (or equivalently $H_\parallel$) and $T < T_{\mathrm{BG}}(H_\parallel, 0)$. Here, R_c is a scaling parameter comparable to R_0, and, for f fixed, $\theta_c(T)$ is determined by fitting $R = R_c(\tan\theta - \tan\theta_c)^{1/2}$ to the data. In Fig. 2, the arrow indicates θ_c obtained in this way. The inset of Fig. 5 shows $t(H_\parallel, H_\perp) \equiv [T_{\mathrm{BG}}(H_\parallel, 0) - T_{\mathrm{BG}}(H_\parallel, H_\perp)]/T_{\mathrm{BG}}(H_\parallel, 0)$ as a function of $H_\perp$, where $T_{\mathrm{BG}}(H_\parallel, H_\perp)$ is obtained through the inversion of θ_c and T. It turns out that $t(H_\parallel, H_\perp)$ is independent of $H_\parallel$. The solid line shown in the inset is a fit to the data following $t(H_\parallel, H_\perp) \sim |H_\perp|^{1/\nu_\perp}$ with $\nu_\perp = 1.0 \pm 0.1$, as recently suggested from numerical simulations [14] and observed in $(\mathrm{K, Ba})\mathrm{BiO_3}$ [15]. Moreover, such a value of $\nu_\perp$ is excellently consistent with the result previously found using the scaling theory of the BG transition at $H_\perp = 0$ [12].

In summary, we demonstrate from transport measurements the stability of the BG phase in a BSCCO single crystal with columnar defects, when **H** is tilted $\theta \leq \theta_c$ away from the column direction. We explain the critical behavior of the linear resistivity on the basis of the CIC transition of kink chains right above θ_c, as predicted in 1 + 1 dimensions for one-dimensional correlated disorder. This implies that the appearance of the TME is concomitant with the vanishing of the linear resistivity at θ_c. As a consequence, our results support the scenario for a usual BG-to-liquid transition in irradiated BSCCO in contrast to a puzzling two-stage BG-to-liquid transition recently observed in untwinned YBCO with columnar defects [8].

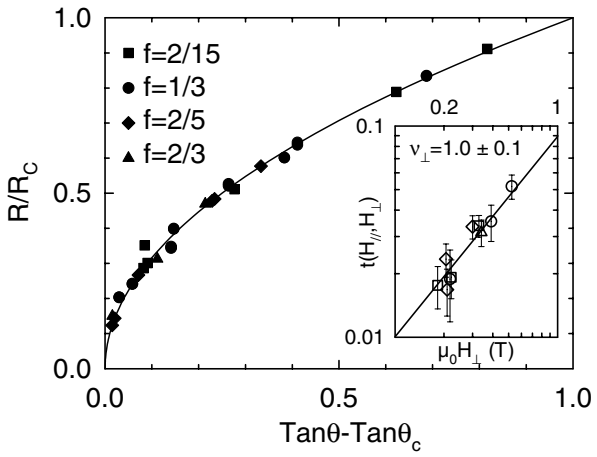

FIG. 5. Critical behavior of the linear resistance for different values of f and T. The curved line is a fit to the data using $R = R_c(\tan\theta - \tan\theta_c)^{1/2}$ in accordance with a CIC transition scenario. Inset: angular dependence of the Bose glass transition. The solid line is a fit of $T_{\mathrm{BG}}(H_\parallel, 0) - T_{\mathrm{BG}}(H_\parallel, H_\perp) \sim |H_\perp|^{1/\nu_\perp}$ with $\nu_\perp = 1.0 \pm 0.1$ to the data; the point $(0, 0)$ is included.

[1] G. Blatter *et al.,* Rev. Mod. Phys. **66**, 1125 (1994).
[2] D. R. Nelson and V. M. Vinokur, Phys. Rev. B **48**, 13 060 (1993).
[3] T. Hwa *et al.,* Phys. Rev. Lett. **71**, 3545 (1993).
[4] M. P. A. Fisher *et al.,* Phys. Rev. B **40**, 546 (1989).
[5] N. Hatano and D. R. Nelson, Phys. Rev. B **56**, 8651 (1997).
[6] T. Hwa, D. R. Nelson, and V. M. Vinokur, Phys. Rev. B **48**, 1167 (1993).
[7] D. Feinberg and C. Villard, Phys. Rev. Lett. **65**, 919 (1990); L. Balents and D. R. Nelson, Phys. Rev. B **52**, 12951 (1995).
[8] A. W. Smith *et al.,* Phys. Rev. B **63**, 064514 (2001).
[9] M. Oussena *et al.,* Phys. Rev. Lett. **76**, 2559 (1996); A. A. Zhukov *et al.,* Phys. Rev. B **56**, 3481 (1997); I. M. Obaidat *et al.,* Phys. Rev. B **56**, R5774 (1997).
[10] A. A. Zhukov *et al.,* Phys. Rev. Lett. **83**, 5110 (1999); Y. V. Bugoslavsky *et al.,* Phys. Rev. B **56**, 5610 (1997).
[11] F. Steinmeyer *et al.,* Europhys. Lett. **25**, 459 (1994); S. Koleśnik *et al.,* Phys. Rev. B **54**, 13 319 (1996).
[12] J. C. Soret *et al.,* Phys. Rev. B **61**, 9800 (2000).
[13] A. Ruyter *et al.,* Physica (Amsterdam) **225C**, 235 (1994).
[14] J. Lidmar and M. Wallin, Europhys. Lett. **47**, 494 (1999).
[15] T. Klein *et al.,* Phys. Rev. B **61**, R3830 (2000).